Research Article | Vol. 10, No. 11 / 1 November 2019 / Biomedical Optics Express 5989
Biomedical Optics EXPRESS

Optical coherence tomography for *in vivo* imaging of endocardial to mesenchymal transition during avian heart development

KATHERINE COURCHAINE AND SANDRA RUGONYI*

Department of Biomedical Engineering, Oregon Health & Science University, 3303 SW Bond Ave. Mail/Code:CH13B, Portland, OR 97239, USA
rugonyis@ohsu.edu

Abstract: The endocardial to mesenchymal transition (EndMT) that occurs in endocardial cushions during heart development is critical for proper heart septation and formation of the heart's valves. In EndMT, cells delaminate from the endocardium and migrate into the previously acellular endocardial cushions. Optical coherence tomography (OCT) imaging uses the optical properties of tissues for contrast, and during early development OCT can differentiate cellular versus acellular tissues. Here we show that OCT can be used to non-invasively track EndMT progression *in vivo* in the outflow tract cushions of chicken embryos. This enables *in vivo* studies to elucidate factors leading to cardiac malformations.

1. Introduction

Embryonic heart development is susceptible to diverse genetic and environmental factors that can lead to cardiac malformations and deficiencies. However, how these factors lead to congenital heart disease (cardiac defect(s) present in the baby at birth) is not fully understood. During early cardiac development, the heart has a tubular shape and its tissues are composed of three distinct layers: endocardium, cardiac jelly, and myocardium. The endocardium is a monolayer of endocardial cells that lines the heart inner surfaces, and is in contact with blood. The myocardium is the outer layer of the heart, is composed of myocardial cells, and starts to cyclically contract as soon as the tubular heart is formed. In between the endocardium and myocardium, there is a layer of initially acellular extracellular matrix components called the cardiac jelly. Optical coherence tomography (OCT) imaging can differentiate these three cardiac layers due to the different optical properties of cells versus the semi-transparent extracellular matrix [1,2,3]. OCT can acquire *in vivo* high resolution images (even < 2 μm resolution in some systems) up to a depth of 1–2mm into embryonic tissues, which is sufficient to image the whole beating tubular heart at early stages of development [3,4,5,6]. There is a trade-off between image resolution and imaging depth, with more depth achieved at the cost of lower resolution, and thus the configuration to choose is dictated by the questions being asked. OCT has been extensively used in diverse studies to image avian embryos and their hearts at early developmental stages [7,8] to understand how environmental factors affect early heart formation [9,10,11,12]. Furthermore, since OCT is a non-contact, non-invasive imaging modality, it allows for longitudinal studies of heart development.

Endocardial to mesenchymal transition (EndMT) is the process by which endocardial cells delaminate from the endocardium, develop a mesenchymal phenotype, and migrate into the cardiac jelly. In the developing heart, EndMT takes place on endocardial cushions, which are regions of thicker cardiac jelly. During EndMT, transforming growth factor beta and bone morphogenetic protein signaling prompt the loss of cell-cell adhesion molecules in the endocardium and the activation of endocardial cells [13]. Activated cells transition to an elongated, motile, invasive phenotype; migrate into the cardiac jelly; and begin to express hallmark proteins characteristic of

#376865 https://doi.org/10.1364/BOE.10.005989
Journal © 2019 Received 2 Sep 2019; revised 20 Oct 2019; accepted 28 Oct 2019; published 1 Nov 2019

Biomedical Optics EXPRESS

mesenchymal cells [14]. In the outflow tract of the heart, these newly formed mesenchymal cells, along with cells from the neural crest and the secondary heart field, continue to migrate and proliferate into the cushions, and drive critical endocardial cushion remodeling and maturation. This remodeling culminates in the development of endocardial cushions into mature valves and septa [13,14,15], which are prone to structural anomalies in humans [14,16]. Several studies have shown that congenital heart valve malformations, as well as some cardiac septal defects and malposition of the great arteries, originate from abnormal EndMT and cushion development [15,17,18]. Therefore EndMT is at the forefront of developmental processes being scrutinized for their role in the pathogenesis of congenital heart disease.

Many studies have been performed in order to discover the genetic and molecular signaling pathways involved in EndMT, e.g., [18,19,20,21,22]. Several studies have also pointed to flow-mediated signaling pathways as key drivers of EndMT, e.g., [23,24,25,26,27,28,29,30]. In particular, altered hemodynamics are known to cause congenital heart defects, and it is therefore desirable to understand in more detail how perturbations in flow affect EndMT such that valve and septa formation are disrupted. Moreover, other environmental perturbations such as excess ethanol or glucose can also lead to flow perturbations that compound the detrimental effects of their toxicity [9,10,11], reinforcing the need to study the accompanying alterations in blood flow dynamics as potential mechanisms leading to malformations. Efforts have therefore been directed at perturbing blood flow in chicken and zebrafish models, quantifying flow perturbations, and determining effects on EndMT by counting the number of cells in cushions through histology or immunohistochemistry methods [23,24,31]. The primary downside to these otherwise amazing studies is that histology and immunohistochemistry methods both require the embryo to be sacrificed, so that EndMT in an embryo can only be examined at a single point in time, post-intervention and post-hemodynamic quantification. While many embryos can be sacrificed at multiple time points to determine EndMT progression, it is desirable to follow specific embryos through time, ideally tracking both hemodynamic changes and the progression of EndMT, to fully understand how hemodynamics and other factors regulate the population and development of endocardial cushions.

We propose here OCT as a tool to longitudinally study the progression of EndMT *in vivo*. In OCT, the backscatter of a light beam directed at a sample is measured using light interferometry, and the native contrast between tissue layers is displayed in the resulting tomographic images (Fig. 1). The penetration depth of the light beam (a couple of millimeters in embryonic tissue) is

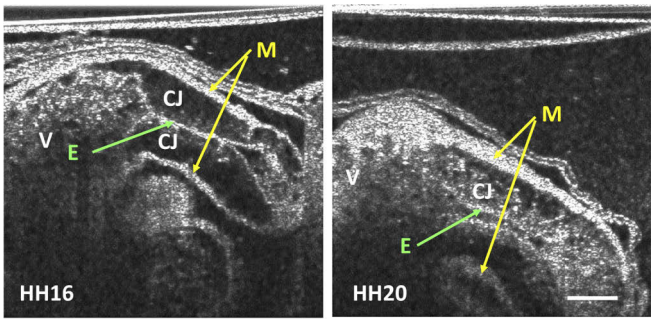

Fig. 1. Embryonic chick outflow tract cushions visualized using OCT. The same embryonic outflow tract was imaged and shown here at HH16 and HH20. Endocardial cushions are clearly delineated by visible endocardial (green arrow) and myocardial (yellow arrow) layers. Please note that at HH16 the cushions have almost no cells, while at HH20 there is a significant increase in cushion cell density. E: endocardium; M: myocardium; CJ: cardiac jelly (endocardial cushions); V: ventricle. Scale bar = 200 μm.

Biomedical Optics EXPRESS

sufficient to visualize the outflow tract cushions of avian embryos for about a day following the onset of EndMT. Furthermore, in addition to collecting structural images, we can simultaneously measure the blood velocity in the direction of the OCT light beam by calculating the Doppler phase shift between scan lines (Doppler OCT), enabling detailed studies of the influence of flow on EndMT progression. Here we present the use of OCT imaging to non-invasively track EndMT progression *in vivo* in the outflow tract cushions of chicken embryos.

2. Methods

Fertilized white Leghorn eggs were incubated blunt end-up at 39°C and approximately 80% humidity for approximately 2 days. Eggs were then windowed by removing a small portion of the shell over the air sac and removing the vitelline membrane over the embryo. Embryos were then staged according to Hamburger-Hamilton stages of avian development [32] as a starting point, and subsequently tracked by hours of incubation. The windows were then sealed with a small Saran Wrap square held in place with Elmer's glue stick, and the eggs returned to the incubator when they were not being imaged.

Images were taken every hour during the day, for as long as an embryo's outflow tract was visible, using our spectral domain OCT imaging system (ThorLabs Telesto III, 1300 nm, at 76kHz, and 580 A-scans). Longitudinal sections of the heart outflow tract were selected so that the imaging plane approximately passed through the center of the heart tube. Imaging plane selection in our OCT system was facilitated by a video camera showing a magnified image of the embryo and its heart that allowed precise positioning of the OCT scanning line that, together with the vertical direction, defined the image acquisition plane. We could image the heart outflow tract until about 3.5–4.5 days of incubation. At each imaging time point, a minimum of one cardiac cycle was captured in a series of B-scans (2D images over time). During the stages of development examined here, a longitudinal OCT scan of the outflow tract was able to capture a distinct endocardial layer, an increasingly cell-populated cardiac jelly, and the myocardial layer (see Fig. 1).

OCT raw data was converted to grayscale structural images (2.68 μm/pixel) and image blobs in the outflow tract cushions (which approximate cushion cells) were counted using in-house MATLAB routines (The MathWorks, Inc. R2019a) as follows. Three points in the cardiac cycle were chosen from sequential OCT outflow tract images: one image when the heart outflow tract was fully contracted, and two when the outflow tract was partly contracted, and enough endocardial cushion was visible to appreciate cell/blob distributions. These images were cropped to the area of the visible upper cushion between the endocardium and the myocardium by manually outlining the area of interest (Fig. 2(A)). The cropped area was then filtered to produce a binary image from which cells could be easily counted. To this end, first the original cropped image was adjusted, and a copy of the image was made in which high intensity areas (cells) were dilated. The intensity of the cropped image was then subtracted from the intensity of the dilated copy so that cells were 'outlined' in this new image. The image with cell/blob outlines was then subtracted from the original cropped image in order to thoroughly discretize the cells. This latter image was binarized, and cell regions (separate clusters of bright pixels) were counted using MATLAB's Blob Analysis function (Fig. 2(B) and (C)). For each hourly time point, the number of cells counted, normalized to the area of the cropped section, was averaged between the three image frames chosen to minimize noise and processing uncertainties. Resulting data was then plotted versus acquisition time to display ENdMT progression from day 2 (HH13).

Biomedical Optics EXPRESS

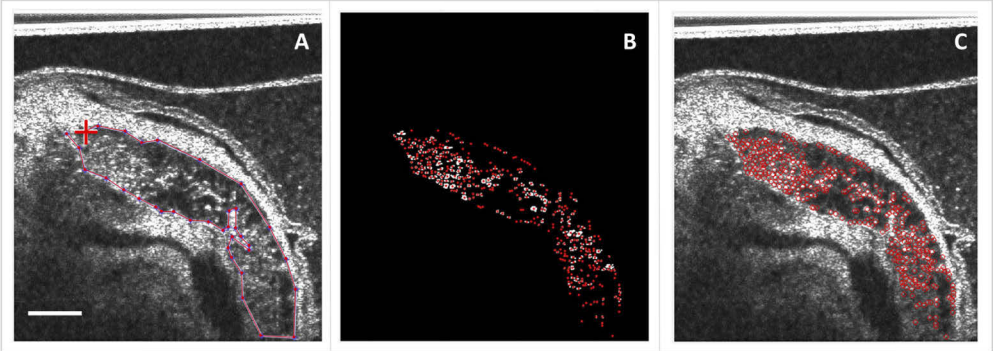

Fig. 2. Semi-automatic cell/blob counting in an HH18 embryo. **A)** The area of interest (upper OFT cushion) is manually selected (outlined) by the user. **B)** The selected area is binarized and MATLAB's Blob Analysis function is used to identify individual cells. **C)** Counted cells/blobs are shown circled on the original OCT image. Cell counts over the developmental stages considered ranged from about 50 to 500 in the cushion area imaged. Scale bar = 170 μm.

3. Results and discussion

We first validated our procedure to count blobs from the cardiac cushion region to approximate quantification of cushion cells and cell density. To ensure that our counting algorithm consistently captured blobs, we imaged the same heart with different OCT settings, but without changing the acquisition imaging plane. We performed several consecutive B-scans changing the number of A-scans (lines) that generated the B-scan, while spanning the same total length. We imaged the heart outflow tract using 580, 1000, 2000, and 5000 A-scans per B-scan. Results showed that changing the number of A-scans did not affect the blob count significantly and thus images could be acquired with as little as 580 A-scans per B-scan without affecting accuracy. Furthermore, we found that differences in blobs counted from the same embryo ($n = 2$) as A-scan numbers per B-scan were changed (in different patterns and including repetitions) were less than 15%, indicating that the blob counting algorithm was consistent.

We used OCT to image the heart outflow tract of 10 chicken embryos starting around HH13, or about day 2 of incubation until approximately day 4. Please note, however, that due to imaging timing and operator-intensive workflow (eggs had to be taken out from the incubator, imaged, and put back in the incubator every hour), there were gaps in image data acquisition (typically about 12 hrs, consistent with lack of imaging overnight). Because data acquisition started at different times during the day, some embryos were only minimally scanned (< 8 time-points) during EndMT progression.

To achieve greater consistency in quantifying endocardial cushion cell density, we averaged results from three frames over the cardiac cycle. This averaging was done to reduce uncertainties introduced by the blob-counting algorithm itself, but also to account for imaging uncertainties and variables. One of the primary limitations of the method presented lies in the consistency of the area scanned and selected for counting. Because the outflow tract is curved in the three-dimensional space, it was impossible to get a perfectly centered longitudinal cross section along the length of the outflow tract tube; the location of the scan also varied slightly from time point to time point (the one-hour interval between imaging sessions) since the embryo was transferred back and forth between the incubator and the imaging stage. Moreover, the endocardial cushion area that was visible varied over the cardiac cycle, as the myocardial tube dynamically expanded and contracted, 'squeezing' the cardiac jelly of the endocardial cushions with each contraction. The dynamic, cyclic contraction of the myocardium rendered the number

Biomedical Optics EXPRESS

of visible (countable) endocardial cushion blobs/cells different from frame to frame. Finally, some embryos had a more irregular endocardial surface than others, which made discerning where to crop the cardiac jelly image difficult. By averaging three frames for each time point, we could mitigate some of these errors and uncertainties.

While we started imaging the embryo heart outflow tract around HH13, EndMT did not start until around HH17. Between approximately 2 and 3 days of incubation, the endocardial cushions were small and not well developed, and the endocardial cushion cell counts were very noisy. Errors and uncertainties in identifying and quantifying cells in this period were amplified by the small dimensions of the cushions themselves. Performing the imaging and quantification starting at day 2, however, allowed us to detect and follow the initiation and development of EndMT in the outflow tract endocardial cushions.

We found that between about 3 and 4 days of incubation (approximately HH17 and later), a very consistent trend in the quantified endocardial cushion cell density over time emerged. The noisy earlier pattern (day 2 to 3) gave way to a consistent linear increase in blob counts per unit area. Furthermore, the slope of the trend line of endocardial cushion cell density over time was highly consistent among embryos (Fig. 3, Table 1). This consistency indicates that, in normal embryonic hearts, there is little biological variation when it comes to outflow tract endocardial cushion population. Thus EndMT is likely a highly regulated process. This is not surprising given that proper endocardial cushion development is essential for the morphological changes that follow (valve formation and cardiac septation) and that give rise to the fully formed heart.

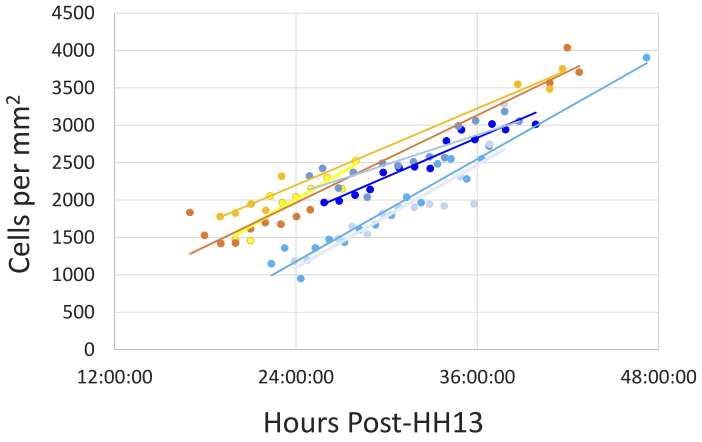

Fig. 3. Quantification of cells per unit area over time in the outflow tract cushions of chicken embryos. Individual data and trend lines are shown for 7 normal embryos for the period during which EndMT is progressing. Data points and trend lines are color-coded by embryo. HH13 refers to Hamburger-Hamilton stage 13, which corresponds to about 2 days of incubation.

Previous studies have shown that the rate of EndMT in endocardial cushions is altered following different interventions, including alterations in blood flow conditions [24]. Those studies, however, were performed by inducing perturbations and then collecting and fixing the embryos to analyze cushion cell population. The advantage of our cell density imaging and quantification technique is that OCT allows for longitudinal visualization of the dynamics of cell population in the endocardial cushions *in vivo*, while enabling quantification of blood flow dynamics in the heart outflow tract around the cushions. In the future, the technique could be applied to determine how rates of cell population in the outflow tract are altered by different interventions, providing a dynamic tool to investigate the origins of congenital heart disease.

Biomedical Optics EXPRESS

Table 1. Embryo statistics for cushion cell density measurements during EndMT period. Time points considered were >15 hours past HH13. Number of cushion cell density data points, R^2 value of linear regression of cell density versus time, and slope of linear trend lines. Only embryos that had 8 or more measurements during the EndMT period were included.

Number of measurements	R^2	Slope
9	0.84	2855
12	0.94	2341
8	0.98	2048
14	0.93	2093
15	0.74	1576
14	0.80	2759
16	0.95	2742

4. Conclusions

We are very excited to present OCT as a viable non-invasive method for the longitudinal study of endocardial to mesenchymal transition (EndMT) in endocardial cushions. The ability to track overall cushion cell population and quantify blood flow dynamics, from the same embryo is invaluable, particularly in studies aiming at characterizing the effects of early developmental dysregulation. In this study we have shown the feasibility of the presented OCT imaging strategy to quantify EndMT progression. Future development of more precise cell counting algorithms could improve quantification accuracy. We envision that interventions that alter endocardial cushion EndMT will cause significant changes in the cell population curves over time, which can be characterized by the strategy presented (e.g., changes in the slope of trend lines). Further, this characterization will allow us to better understand how diverse interventions lead to congenital heart defects.

Funding

National Heart, Lung, and Blood Institute (HL094570); Medical Research Foundation.

Acknowledgements

We would like to acknowledge the help of Graham Rykiel in preparing embryos for imaging.

Disclosures

The authors declare no conflicts of interest.

References

1. I. V. Larina, K. V. Larin, M. J. Justice, and M. E. Dickinson, "Optical Coherence Tomography for live imaging of mammalian development," Curr. Opin. Genet. Dev. **21**(5), 579–584 (2011).
2. S. Rugonyi, C. Shaut, A. Liu, K. Thornburg, and R. K. Wang, "Changes in wall motion and blood flow in the outflow tract of chick embryonic hearts observed with optical coherence tomography after outflow tract banding and vitelline-vein ligation," Phys. Med. Biol. **53**(18), 5077–5091 (2008).
3. M. Midgett, V. K. Chivukula, C. Dorn, S. Wallace, and S. Rugonyi, "Blood flow through the embryonic heart outflow tract during cardiac looping in HH13–HH18 chicken embryos," J. R. Soc., Interface **12**(111), 20150652 (2015).
4. R. Yelin, D. Yelin, W. Y. Oh, S. H. Yun, C. Boudoux, B. J. Vakoc, B. E. Bouma, and G. J. Tearney, "Multimodality optical imaging of embryonic heart microstructure," J. Biomed. Opt. **12**(6), 064021 (2007).
5. M. W. Jenkins, D. C. Adler, M. Gargesha, R. Huber, F. Rothenberg, J. Belding, M. Watanabe, D. L. Wilson, J. G. Fujimoto, and A. M. Rollins, "Ultrahigh-speed optical coherence tomography imaging and visualization of the embryonic avian heart using a buffered fourier domain mode locked laser," Opt. Express **15**(10), 6251–6267 (2007).
6. J. Manner, L. Thrane, K. Norozi, and T. M. Yelbuz, "High-resolution in vivo imaging of the cross-sectional deformations of contracting embryonic heart loops using optical coherence tomography," Dev. Dyn. **237**(4), 953–961 (2008).

Biomedical Optics EXPRESS

7. M. W. Jenkins, L. Peterson, S. Gu, M. Gargesha, D. L. Wilson, M. Watanabe, and A. M. Rollins, "Measuring hemodynamics in the developing heart tube with four-dimensional gated Doppler optical coherence tomography," J. Biomed. Opt. **15**(6), 066022 (2010).
8. M. Jenkins, M. Watanabe, and A. Rollins, "Longitudinal imaging of heart development with optical coherence tomography," IEEE J. Sel. Top. Quantum Electron. **18**(3), 1166–1175 (2012).
9. G. Karunamuni, S. Gu, Y. Q. Doughman, L. M. Peterson, K. Mai, Q. McHale, M. W. Jenkins, K. K. Linask, A. M. Rollins, and M. Watanabe, "Ethanol exposure alters early cardiac function in the looping heart: a mechanism for congenital heart defects?" American Journal of Physiology-Heart and Circulatory Physiology **306**(3), H414–H421 (2014).
10. L. M. Peterson, S. Gu, G. Karunamuni, M. W. Jenkins, M. Watanabe, and A. M. Rollins, "Embryonic aortic arch hemodynamics are a functional biomarker for ethanol-induced congenital heart defects [Invited]," Biomed. Opt. Express **8**(3), 1823–1837 (2017).
11. T. Lawson, D. Scott-Drechsel, V. Chivukula, S. Rugonyi, K. Thornburg, and M. Hinds, "Hyperglycemia Alters the Structure and Hemodynamics of the Developing Embryonic Heart," J. Cardiovasc. Dev. Dis. **5**(1), 13 (2018).
12. M. Midgett, S. Goenezen, and S. Rugonyi, "Blood flow dynamics reflect degree of outflow tract banding in Hamburger-Hamilton stage 18 chicken embryos," J. R. Soc., Interface **11**(100), 20140643 (2014).
13. K. Courchaine, G. Rykiel, and S. Rugonyi, "Influence of blood flow on cardiac development," Prog. Biophys. Mol. Biol. **137**, 95–110 (2018).
14. H. Gong, X. Lyu, Q. Wang, M. Hu, and X. Zhang, "Endothelial to mesenchymal transition in the cardiovascular system," Life Sci. **184**, 95–102 (2017).
15. T. D. Camenisch, R. B. Runyan, and R. R. Markwald, "Molecular Regulation of Cushion Morphogenesis," Chapter 6.1 in *Heart Development and Regeneration* (Academic Press, 2010) pp. 363–387.
16. D. Srivastava and E. N. Olson, "A genetic blueprint for cardiac development," Nature **407**(6801), 221–226 (2000).
17. B. P. T. Kruithof, S. N. Duim, A. T. Moerkamp, and M.-J. Goumans, "TGFβ and BMP signaling in cardiac cushion formation: Lessons from mice and chicken," Differentiation (Oxford, U. K.) **84**(1), 89–102 (2012).
18. A. L. P. Tavares, M. E. Mercado-Pimentel, R. B. Runyan, and G. T. Kitten, "TGFβ-mediated RhoA expression is necessary for epithelial-mesenchymal transition in the embryonic chick heart," Dev. Dyn. **235**(6), 1589–1598 (2006).
19. A. D. Person, R. J. Garriock, P. A. Krieg, R. B. Runyan, and S. E. Klewer, "Frzb modulates Wnt-9a-mediated β-catenin signaling during avian atrioventricular cardiac cushion development," Dev. Biol. (Amsterdam, Neth.) **278**(1), 35–48 (2005).
20. Y. Bai, J. Wang, Y. Morikawa, M. Bonilla-Claudio, E. Klysik, and J. F. Martin, "Bmp signaling represses Vegfa to promote outflow tract cushion development," Development (Cambridge, U. K.) **140**(16), 3395–3402 (2013).
21. H. Zhang, A. von Gise, Q. Liu, T. Hu, X. Tian, L. He, W. Pu, X. Huang, L. He, C.-L. Cai, F. D. Camargo, W. T. Pu, and B. Zhou, "Yap1 Is Required for Endothelial to Mesenchymal Transition of the Atrioventricular Cushion," J. Biol. Chem. **289**(27), 18681–18692 (2014).
22. A. L. P. Tavares, J. A. Brown, E. C. Ulrich, K. Dvorak, and R. B. Runyan, "RUNX2-I is an early regulator of epithelial-mesenchymal cell transition in the chick embryo," Dev. Dyn. **247**(3), 542–554 (2018).
23. V. Menon, J. Eberth, R. Goodwin, and J. Potts, "Altered Hemodynamics in the Embryonic Heart Affects Outflow Valve Development," J. Cardiovasc. Dev. Dis. **2**(2), 108–124 (2015).
24. M. Midgett, C. S. López, L. David, A. Maloyan, and S. Rugonyi, "Increased Hemodynamic Load in Early Embryonic Stages Alters Endocardial to Mesenchymal Transition," Front. Physiol. **8**, 56 (2017).
25. J. Vermot, A. S. Forouhar, M. Liebling, D. Wu, D. Plummer, M. Gharib, and S. E. Fraser, "Reversing Blood Flows Act through klf2a to Ensure Normal Valvulogenesis in the Developing Heart," PLoS Biol. **7**(11), e1000246 (2009).
26. E. Heckel, F. Boselli, S. Roth, A. Krudewig, H.-G. Belting, G. Charvin, and J. Vermot, "Oscillatory Flow Modulates Mechanosensitive klf2a Expression through trpv4 and trpp2 during Heart Valve Development," Curr. Biol. **25**(10), 1354–1361 (2015).
27. L. M. Goddard, A.-L. Duchemin, H. Ramalingan, B. Wu, M. Chen, S. Bamezai, J. Yang, L. Li, M. P. Morley, T. Wang, M. Scherrer-Crosbie, D. B. Frank, K. A. Engleka, S. C. Jameson, E. E. Morrisey, T. J. Carroll, B. Zhou, J. Vermot, and M. L. Kahn, "Hemodynamic Forces Sculpt Developing Heart Valves through a KLF2-WNT9B Paracrine Signaling Axis," Dev. Cell **43**(3), 274–289.e5 (2017).
28. S. M. Ford, M. T. McPheeters, Y. T. Wang, P. Ma, S. Gu, J. Strainic, C. Snyder, A. M. Rollins, M. Watanabe, and M. W. Jenkins, "Increased regurgitant flow causes endocardial cushion defects in an avian embryonic model of congenital heart disease," Congenital Heart Disease **12**(3), 322–331 (2017).
29. R. E. Poelmann and A. C. Gittenberger-de Groot, "Hemodynamics in Cardiac Development," J. Cardiovasc. Dev. Dis. **5**(4), 54 (2018).
30. V. Menon, J. F. Eberth, L. Junor, A. J. Potts, M. Belhaj, D. J. Dipette, M. W. Jenkins, and J. D. Potts, "Removing vessel constriction on the embryonic heart results in changes in valve gene expression, morphology, and hemodynamics," Dev. Dyn. **247**(3), 531–541 (2018).
31. J. J. Hsu, V. Vedula, K. I. Baek, C. Chen, J. Chen, M. I. Chou, J. Lam, S. Subhedar, J. Wang, Y. Ding, C.-C. Chang, J. Lee, L. L. Demer, Y. Tintut, A. L. Marsden, and T. K. Hsiai, "Contractile and hemodynamic forces coordinate Notch1b-mediated outflow tract valve formation," JCI Insight **4**(10), e124460 (2019).
32. V. Hamburger and H. L. Hamilton, "A series of normal stages in the development of the chick embryo," Dev. Dyn. **195**(4), 231–272 (1992).